J. Plasma Physics (2013), vol. 79, part 2, pp. 189–196. © Cambridge University Press 2012
doi:10.1017/S0022377812000839

Shukla–Eliasson attractive force: Revisited

M. AKBARI-MOGHANJOUGHI

Department of Physics, Faculty of Sciences, Azarbaijan University of Shahid Madani, 51745-406, Tabriz, Iran
(m_akbari@azaruniv.edu)

(Received 21 July 2012; revised 1 August 2012; accepted 3 August 2012; first published online 30 October 2012)

Abstract. By investigating the dielectric response of the Fermi–Dirac plasma in the linear limit and evaluating the electrostatic potential around the positive stationary test charge, we find that the Shukla–Eliasson attractive force is present for the plasma density range expected in the interiors of large planets for a wide range of plasma atomic number. This research, which is based on the generalized electron Fermi-momentum, further confirms the existence of the newly discovered Lennard-Jones-like attractive potential and its inevitable role in plasma crystallization in the cores of planets. Moreover, it is observed that the characteristics of the attractive potential are strongly sensitive to the variation of plasma density and composition. Current research can also have applications in the study of strong laser-matter interactions and inertially confined plasmas.

1. Introduction

Miniaturization in technology on one hand and interest in astrophysical phenomena on the other have motivated a great deal of enthusiasm toward the study of quantum plasmas. In a series of papers, Fowler (1926), Chandrasekhar (1931), Chandrasekhar (1933), Bohm and Pines (1953), Pines (1953), and Levine and Roos (1962) have founded the concepts of relativistic-degeneracy and quantum plasma theories. Recent developments of quantum hydrodynamic (QHD) (Haas et al. 2003; Manfredi 2005) and spin-1/2 quantum magnetohydrodynamic (QMHD) models (Marklund and Shukla 2006; Marklund and Brodin 2007; Brodin et al. 2008) based on the Wigner–Poisson and Schrödinger–Poisson formulation (e.g., see Haas 2011) have opened a new area of research in the field of cold ionized plasmas. QHD theories can be used to evaluate the dynamics of spin-1/2 electron-hole systems such as semiconductors (Markowich et al. 1990; Gardner 1994) and nanostructured materials (Shukla and Eliasson 2010). Recent studies based on the QHD model have revealed that the particle non-locality feature introduced into the quantum plasma model due to the Bohm force is a new feature present only in Fermi fluid models and can introduce additional critical quantum effects in the collective dynamics of the Fermi–Dirac plasmas. Quantum plasmas have much reduced average inter-particle distances compared with that in the classical counterparts. It has also been shown that the particle diffraction effect in the quantum plasma can lead to new multistream plasma instabilities not encountered in ordinary classical plasmas (Manfredi and Haas 2001). Extended QHD formalisms have recently appeared for magnetized and unmagnetized cases taking into account the relativistic spin-orbit interaction of Fermi–Dirac particles ubiquitous in strong laser-matter interactions and astrophysical dense plasmas (Asenjo et al. 2011; Mendonça 2011; Haas et al. 2012).

Applications of QMHD in quantum plasmas, on the other hand, reveal that dynamics of the Fermi spin-1/2 plasma is fundamentally affected by the pressure caused due to electron spin and orbit magnetization (Brodin and Marklund 2007; Marklund et al. 2008). Furthermore, it has been shown that the magnetization in quantum plasmas can give rise to distinct degeneracy regimes (Akbari-Moghanjoughi 2010) and remarkable behavior for spin-induced nonlinear waves (Akbari-Moghanjoughi 2011a). One of the distinguished manifestations of electron quantum diffraction effect in degenerate plasmas is the plasma dielectric response to the external electromagnetic perturbations. The plasma dielectric susceptibility for unmagnetized and magnetized quantum plasmas has been recently investigated by many authors. The new findings indicate the critical influence of quantum effects on the Debye shielding in Fermi plasmas (Salimullah et al. (2009). As a fundamental problem, there has been many previous investigations on the potential around a test charge in variety of plasma environments (Stenflo et al. 1973; Tegeback and Stenflo 1975; Shukla et al. 2006; Stenflo and Shukla 2010). More recently, by evaluating the electrodynamic potential of a moving test charge in a quantum plasma, the modified Debye–Hückel (DH) potential, i.e., the ordinary DH potential coupled with an oscillatory term, has been found in quantum plasmas (Shukla and Eliasson 2008). Such modified DH potential, particularly caused by the presence of electron degeneracy, interaction energies, and the electron non-locality effect, has been shown to lead to a new type of the Lennard-Jones-like attractive force with a pronounced potential valley near the test particle (Shukla and Eliasson 2012). The

https://doi.org/10.1017/S0022377812000839 Published online by Cambridge University Press

discovery of such new force in quantum plasmas has fundamental significance for plasma coupling, crystallization, and quantum transport effects in dense plasmas. The introduction of such attractive force, which brings the ions closer together, may even lead to breakthroughs in semiconductor, supercomputing, and nanotechnology sciences.

The astrophysical applications of the quantum hydrostatic model became apparent since the pioneering work of Chandrasekhar (1931, 1939, 1953) on the relativistic degeneracy. Due to the change in the equation of state of the electron degeneracy pressure in the relativistic degeneracy limit, a fundamental limit on white dwarf mass has been discovered (Chandrasekhar 1984) and distinct features have been shown to exist in the QHD wave dynamics of the ultrarelativistic Fermi–Dirac plasmas (Akbari-Moghanjoughi 2011b). On the other hand, the application of QMHD model suggests some large-scale effects, such as modification on the well-known Jeans criteria (Lundin et al. 2008), due to the presence of electron spin and orbital magnetizations. Therefore, it is appealing to examine the effect of relativistic degeneracy on quantum plasma shielding and its dielectric response. In the relativistically degenerate Fermi–Dirac plasma, Salpeter (1961) has evaluated the effects of a variety of interaction potentials such as Coulomb lattice-energy, Thomas–Fermi distribution, electron-exchange, and correlation on stellar hydrostatic stability for a wide range of relativity parameters, and has found more significant contribution due to the Coulomb lattice energy compared with other interaction effects. Such a plasma interaction effect, although being a few percent of the dominant electron degeneracy effect, can give rise to crystallization of the Fermi–Dirac plasma in superdense stellar cores. In this paper we aim at examining the linear plasma response and the potential of a test charge due to the presence of Coulomb interactions and the Bohm force in the relativistically degenerate Fermi–Dirac plasmas for a wide range of relativity parameter (electron number–density). We present a QHD model in Sec. 2 and examine the plasma dielectric constant in linear limit in Sec. 3. Then, in Sec. 4 we calculate the modified Debye–Huckel potential around a stationary positive test charge, and in Sec. 5 we give the parametric description of the associated potential. Finally, in Sec. 6 we make numerical evaluation of the calculated potential based on independent plasma parameters, and in Sec. 7 we draw our conclusions.

2. Quantum hydrodynamics model

In this model we consider a plasma of non-degenerate stationary ions with charge Z quasineutrally distributed into a completely degenerate Fermi–Dirac electron fluid. The ion thermal energy is neglected compared to the electron Fermi energy (E_{Fe}), hence they are assumed to be static and unperturbed to external simulations compared with light electrons ($m_e/m_i \ll 1$). Furthermore, we use the nearly free electron model neglecting the electron fluid viscosity. The electron viscosity has been shown to becomes dominant in much larger densities such as in neutron–star crusts (Itoh et al. 1987). On the other hand, it is also shown that in quantum plasmas the electron–electron collisions are limited due to the Pauli blocking mechanism (Shukla and Eliasson 2010). In the electron number-density regime, considered in this work ($10^{22} - 10^{26}/\mathrm{cm}^3$), one may also assume infinite plasma conductivity ($\sigma \simeq 10^{22}$), thereby neglecting the ion–electron collision frequency (Nandkumar and Pethick 1984) compared with the characteristic plasma frequencies. Therefore, the hydrodynamic evolution of the Fermi–Dirac electron gas is governed by the following set of equations (Crouseilles et al. 2008), as follows:

$$\begin{aligned}
&\frac{\partial n}{\partial t} + \nabla \cdot (n\mathbf{u}) = 0,\\
&\frac{\partial \mathbf{u}}{\partial t} + (\mathbf{u}\cdot\nabla)\mathbf{u} = e\nabla\phi - \frac{1}{m_e n}\nabla P_G + \frac{\hbar^2}{2m_e^2}\nabla\left[\Delta\sqrt{n}/\sqrt{n}\right],\\
&\Delta\phi(\mathbf{r}) = 4\pi e(n - n_0),
\end{aligned} \tag{2.1}$$

where $\hbar$ and c are the scaled Plank-constant and speed of light in vacuum respectively. Also, P_G is the generalized pressure of plasma composed of electron degeneracy, exchange, and Coulomb interaction pressures, i.e., $P_G = P_d + P_{xc} + P_C$, and n_0 is the unperturbed electron density. Ignoring the negligible ion pressure compared with that of the quantum pressure of electrons, a general form of electron degeneracy pressure for a wide range of plasma density is given as (Chandrasekhar 1939)

$$P_e = \frac{\pi m_e^4 c^5}{3h^3}\{R(2R^2-3)\sqrt{1+R^2} + 3\ln[R+\sqrt{1+R^2}]\}, \tag{2.2}$$

where the Chandrasekhar relativity parameter, R, is related to the Fermi relativistic-momentum via the relation $R = p_{Fe}/m_e c = (n/n_c)^{1/3}$ with $n_c \simeq 5.9 \times 10^{29}\mathrm{cm}^{-3}$ being the normalizing value. Furthermore, a relativistic degeneracy parameter, R_0, may be introduced as $R = R_0(n/n_0)^{1/3}$, where $R_0 = (n_0/n_c)^{1/3}$ with n_0 being the unperturbed equilibrium electron number-density. It can be easily shown that for the degenerate electron pressure represented as a polytropic form of $P = P_0(n/n_0)^{\gamma}$ the values of $\gamma = \{5/3, 4/3\}$ correspond to the degeneracy limits $R = \{0, \infty\}$ of (2.2) as non-relativistic and ultrarelativistic degeneracy limits respectively. The change in equation of state due to the relativistic degeneracy of electrons has been shown to lead to the well-known white dwarf mass limit (Chandrasekhar 1953) and distinct features in nonlinear wave dynamics in the Fermi–Dirac plasmas (Akbari-Moghanjoughi 2010). It can be observed that the polytropic form of the Chanrasekhar pressure approaches nicely to the standard Fermi degeneracy pressure for an extremely non-relativistic

https://doi.org/10.1017/S0022377812000839 Published online by Cambridge University Press

number-density range (Akbari-Moghanjoughi 2012a). It is evident that one needs to use the full form of pressure, valid for a wide plasma density range, in order to evaluate the Shukla–Eliasson force and phase separation in dense quantum plasma to be shown present also in the interiors of large planets.

As the plasma becomes denser, the corrections to the equation of state of the plasma due to particle interactions become important. Such interaction terms in the strong coupling plasma limit are due to the electrostatic plasma interactions (Coulomb interactions), electron exchange, electron non-uniform distribution (Thomas–Fermi correction), ion correlation, and some other minor effects (Salpeter 1961). It is known that the plasma coupling parameter, Γ, is inversely proportional to the inter-particle distance, r_{ij}, and the temperature T of plasma species. Hence, with the inter-particle distances being of the same order for ions and electrons in the quasineutrality limit, the coupling parameter for ions is observed to be much larger than that for degenerate electrons, since the interacting electron temperature is of the order of the Fermi-temperature being much higher than the ion thermal temperature ($\Gamma_i \gg \Gamma_e$). The Coulomb attractive potential, being the dominant interaction potential, is the main cause of the crystallization of Fermi–Dirac plasmas under strong coupling conditions. Its dominant effects are well understood in ordinary solids-state matter and are believed to play a fundamental role in the Fermi–Dirac plasmas lattice formation. Calculation of the collective electrostatic energy of crystals with different periodic configurations such as the *fcc* and the *hcp* lattice structures confirm that the Coulomb energy of a lattice is minimally related to the lattice structure (Kittel 1939). Salpeter (1961) , using the spherical non-interacting Wigner–Seitz cell of radius r_0 ($1/n_0 = 4\pi r_0^3/3$), has given an expression for the Coulomb energy of a relativistically degenerate plasma with ions forming a quasi-lattice at very high electron density plasma regime such as in a white dwarf core or neutron star crust. It has been shown that such attractive force persists and even becomes stronger as the value of the relativity parameter or the electron number-density increases. On the other hand, the plasma coupling parameter, which is given by $\Gamma = (Ze)^2/(r_0 k_B T)$, may also be approximated in terms of the relativity parameter as $\Gamma \simeq 0.23 Z^{5/3} R/T_8$, (where T_8 is the plasma temperature in units of 10^8 degrees Kelvin) (Itoh et al. 1987). It is known that the plasma is in liquid form for the coupling parameter range $\Gamma < 178$ and in solid phase beyond this value (Itoh et al. 1987). Hence, it is concluded that for a typical planet core temperature, say 24 000 K for Jupiter core, and a typical relativity parameter of $R \simeq 0.1$, the coupling parameter value exceeds the liquid critical limiting value. Therefore, it is observed that the planet cores for a wide range of plasma atomic number value would be in a quasi-lattice phase. The effects of interaction potential on ion wave dynamics in the Fermi–Dirac plasmas have been investigated recently (Akbari-Moghanjoughi 2012b),

$$P_C = -\frac{8\pi^3 m_e^4 c^5}{h^3}\left[\frac{a_0 Z^{2/3}}{10\pi^2}\left(\frac{4}{9\pi}\right)^{1/3}\right] R^4, \tag{2.3}$$

where Z is the atomic number of ions and h is the Planck constant. It should be noted that the Coulomb pressure presented here only gives a qualitatively right order for $Z^{2/3}(r_0/r_B) \simeq 1$ in the non-relativistic plasma density limit ($10^{25} < n_0/\mathrm{cm}^3 < 10^{27}$), where r_0 and r_B are the Wigner–Seitz and Bohr radiuses respectively. Therefore, in the forthcomming analysis we will confine our analysis to this validity limit which is relevant for the planet core density range. On the other hand, the contribution from the electron exchange may be written as

$$\begin{aligned} P_{xc} = -\frac{2a_0 m_e^4 c^5}{h^3}\Big\{ & \frac{1}{32}(\beta^4+\beta^{-4}) + \frac{1}{4}(\beta^2+\beta^{-2}) \\ & - \frac{3}{4}(\beta^2-\beta^{-2})\ln\beta + \frac{3}{2}(\ln\beta)^2 - \frac{9}{16} \\ & - \frac{R}{3}\left(1+\frac{R}{\sqrt{1+R^2}}\right)\Big[\frac{1}{8}(\beta^3-\beta^{-5}) - \frac{1}{4}(\beta-\beta^{-3}) \\ & - \frac{3}{2}(\beta+\beta^{-3})\ln\beta + \frac{3\ln\beta}{\beta}\Big]\Big\}, \end{aligned} \tag{2.4}$$

where $\beta = R + \sqrt{1+R^2}$. The Coulomb interaction pressure is always negative, whereas the pressure due to electron exchange changes the sign at the relativity parameter value of around $R \simeq 2$ (Akbari-Moghanjoughi 2012b). It should be noted that in the forthcoming calculations we have included the generalized form of the exchange energy, given by Salpeter (1961), instead of that in Shukla and Eliasson (2012), since the generalized exchange energy is valid for a wide electron number-density range. We have further neglected the effect of electron-correlation effect due to the vanishingly small contribution in the considered density regime (Salpeter 1961).

3. Linear dielectric response

In order to obtain the dielectric constant for the present plasma model we use a standard procedure employed by Shukla and Eliasson (2012). The QHD equations given in (3.2) now read as

$$\begin{aligned} & \frac{\partial n}{\partial t} + \nabla\cdot n\mathbf{u} = 0, \\ & \frac{\partial \mathbf{u}}{\partial t} + (\mathbf{u}\cdot\nabla)\mathbf{u} = \frac{e}{m_e}\nabla\phi - c^2\nabla\left[\Psi_d + \Psi_{xc} + \Psi_C\right] \\ & \qquad\qquad + \frac{\hbar^2}{2m_e^2}\nabla\frac{\Delta\sqrt{n}}{\sqrt{n}}, \\ & \Delta\phi(\mathbf{r}) = 4\pi e(n-n_0), \end{aligned} \tag{3.1}$$

where Ψs are the effective plasma potentials defined via the relation

$$\Psi = \frac{1}{m_e}\int \frac{d_R P(R)}{R^3} dR, \quad \nabla\Psi = \frac{1}{m_e}\frac{1}{R^3}\frac{dP(R)}{dR}\nabla R. \tag{3.2}$$

https://doi.org/10.1017/S0022377812000839 Published online by Cambridge University Press

The plasma effective potentials are then given as

$$\Psi_d = \sqrt{1+R_0^2 n^{2/3}},$$

$$\Psi_{xc} = \frac{a_0}{2\pi}\left[R_0 n^{1/3} - \frac{3\sinh^{-1}(R_0 n^{1/3})}{\sqrt{1+R_0^2 n^{2/3}}}\right],$$

$$\Psi_C = -\beta R_0 n^{1/3}, \tag{3.3}$$

with

$$\beta = \frac{2a_0}{5}\left(\frac{2Z}{3\sqrt{\pi}}\right)^{2/3}, \quad a_0 \simeq 1/137. \tag{3.4}$$

To evaluate the linear response of the plasma to harmonic excitations of the form $\propto \exp[i(\mathbf{k}\cdot\mathbf{r}-\omega t)]$, we use the well-known harmonic operators $\nabla \equiv i\mathbf{k}$ and $\partial_t \equiv -i\omega$ to linearize the equation set (3.1). Assuming a small density perturbation around the equilibrium state (i.e., $\mathbf{u}=\mathbf{u_1}$, $\phi=\phi_1$, and $n = n_0 + n_1$ with $n_1 \ll n_0$), we obtain the following equations:

$$-\omega n_1 + \mathbf{k}\cdot\mathbf{u_1} = 0,$$

$$-\omega \mathbf{u_1} = -\frac{\hbar^2}{4m_e^2}k^2\mathbf{k}n_1 - c^2 T\mathbf{k}n_1,$$

$$T = \frac{R_0^2}{3\sqrt{1+R_0^2}} - \frac{\beta}{3}R_0 + \frac{a_0}{2\pi}\left[\frac{R_0}{3} - \frac{R_0}{1+R_0^2} + \frac{R_0^2\sinh^{-1}R_0}{(1+R_0^2)^{3/2}}\right], \tag{3.5}$$

the reduction of which yields the first-order potential perturbation and the electron dielectric susceptibility as

$$\chi_e^{-1} = -\frac{k^2\phi_1}{n_1} = \frac{\hbar^2}{4m_e^2}k^4 + c^2T - \omega^2, \tag{3.6}$$

where χ_e is the dielectric susceptibility related to the dielectric constant as $\epsilon(\omega,\mathbf{k}) = 1+\chi_e$. In the quasistationary limit, we obtain the normalized dielectric constant as (Shukla and Eliasson 2012)

$$\epsilon(0,\mathbf{k}) = 1 + \omega_{pe}^2\left[\frac{\hbar^2}{4m_e^2}k^4 + c^2T\right]^{-1}, \tag{3.7}$$

where $\omega_{pe} = \sqrt{4\pi n_0 e^2/m_e}$ is the electron plasmon frequency. Note that in many recent quantum plasma literature the use of the quantum diffraction parameter, $H = \hbar^2\omega_{pi}^2/(2m_e c^2)$ called the scaled ion-plasmon frequency, has become widespread. The value of this parameter can be approximated as $H \simeq 0.0044\, Z R_0^{3/2}$, which for metallic iron density of $\simeq 10^{23}/\mathrm{cm}^3$ and higher density of our concern ($10^{26}/\mathrm{cm}^3$) with same composition takes the values as $H \simeq 0.00005$ and $H \simeq 0.002$ respectively. However, the corresponding values are much smaller than that suggested previously (Haas et al. 2003) for metallic solids, which is due to the normalization factor used in this work.

4. Phase separation in Fermi–Dirac plasmas

Let us consider a positive stationary test charge in the plasma with Fermi–Dirac degenerate electrons. The shielding of such a test charge is a fundamental property of the plasma and can give useful information about the bound states between ions. The Debye-shielding or the near-field electrostatic potential usually appears as $\phi(r) \propto (1/r)exp(-r/r_d)$, where r_d is the Debye-length and r is the distance from the test charge (Krall and Trivelpeice 1932). In the extreme non-relativistic degeneracy limit the plasma shielding potential can also attribute to a far-field inverse cubic dependence (r^{-3}) from an outside inertial observer point of view (Shukla and Eliasson 2008). Let us for simplicity assume a stationary test charge $Q_T = Q$ located at the origin. It is obvious that analysis can be extended to a moving test charge with velocity $\mathbf{v}_T$ relative to the laboratory frame (Shukla and Eliasson 2008). The Poisson equation in the presence of point-like stationary positive test charge can be written as

$$\Delta\phi(\mathbf{r}) = 4\pi e(n-n_0) - 4\pi Q\delta(\mathbf{r}), \tag{4.1}$$

where $\delta(\mathbf{r})$ is the Dirac delta-function ensuring the localization of the test charge at the origin, i.e., $\delta(\mathbf{0}) = 1$ and $\delta(\mathbf{r}\neq\mathbf{0}) = 0$. Using the Fourier analysis in space, the electrostatic potential around the test charge can be rewritten in the form

$$\phi(\mathbf{r}) = \frac{Q}{2\pi^2}\int \frac{\exp(i\mathbf{k}\cdot\mathbf{r})}{k^2\epsilon(\mathbf{k})}d^3k, \tag{4.2}$$

where $\epsilon(\mathbf{k})$ is the plasma dielectric constant given by (3.6). We then appropriately decompose the integral following the procedure given by Shukla and Eliasson (2012). Therefore, the integral in (4.2) can be decomposed into different parts as follows:

$$\phi(\mathbf{r}) = \frac{Q}{4\pi^2}\int\left[\frac{1+L}{k^2+k_1^2} + \frac{1-L}{k^2+k_2^2}\right]\exp(i\mathbf{k}\cdot\mathbf{r})d^3k, \tag{4.3}$$

where the parameters $k_{1,2}$ and L are given as

$$k_{1,2}^2 = k_0^2\frac{1\mp\sqrt{1-4\alpha}}{2\alpha}, \quad L = \sqrt{1-4\alpha}, \tag{4.4}$$

with the parameters k_0 and α given as

$$\alpha = \frac{\hbar^2\omega_p^2}{4m_e^2c^4T^2}, \quad k_0 = \frac{\omega_p}{c\sqrt{T}}. \tag{4.5}$$

Now, using the condition $\phi(r=\infty) = 0$, and the standard definition

$$\int\frac{\exp(i\mathbf{k}\cdot\mathbf{r})}{k^2+k_{1,2}^2}d^3k = \frac{2\pi^2}{r}e^{-k_{1,2}r}, \tag{4.6}$$

we may write the general solution for the first-order potential perturbation around the test charge as

$$\phi(r) = \frac{Q}{2r}[(1+L)e^{-k_1r} + (1-L)e^{-k_2r}]. \tag{4.7}$$

We then are in a position to evaluate the potential around the test charge in the Fermi–Dirac degenerate plasma with respect to two independent plasma parameters, namely the relativistic degeneracy parameter R_0,

https://doi.org/10.1017/S0022377812000839 Published online by Cambridge University Press

representing the normalized number-density of electrons, and the atomic-number Z, of plasma ions. As it is evident, this can be only done in a numerical scheme presented below. We will present phase separation in the Fermi–Dirac plasma for different values of plasma atomic number using the scaled Bohr-radius $r_s = r_B/r_0$, where $r_B = \hbar^2/m_e e^2$ is the Bohr-radius. This implies the relation $R_0 \approx 0.014\, r_s$ between the degeneracy parameter R_0 and the scaled Bohr-radius r_s.

5. Shukla–Eliasson attractive potential in Fermi–Dirac plasmas

It is evident that for a physical solution to exist, in (4.7), the value of the potential must be real. It can be easily confirmed that for all values of $\alpha > 1/4$ the parameter L is imaginary. Therefore, for $\alpha > 1/4$ (it can be confirmed that the parameter α is always positive), we have $\Re(k_1) = \Re(k_2)$ and $\Im(k_1) = -\Im(k_2)$, hence $k_{1,2} = \Re(k_1) \pm \Im(k_1)$ (Shukla and Eliasson 2012) and the electrostatic potential can be written in the form $\phi(r) = (Q/r)\exp[-\Re(k_2)r]\{\cos[\Re(k_2)r] + \Re(L)\sin[\Im(k_2)r]\}$, where $\Re$ and $\Im$ refer to the real and imaginary parts of the parameter k_2 respectively. This attractive Lennard-Jones-like potential relates to the ion-bound states of the Fermi–Dirac plasma. However, for $\alpha < 1/4$, where the parameter L becomes real-valued, the potential of a test charge reduces to the repulsive Debye–Huckel or Yukawa-type potential. It is important to note that the Shukla–Eliasson force is an elegant manifestation of pure quantum mechanical effect and a consequence of the electron collective quantum behavior, since it disappears in the $\hbar \to 0$ limit. It is also observed that the characteristics of such attractive force depends strongly on the atomic number of plasma ions. As it will be revealed in Sec. 6, our research highlights the importance of quantum tunneling effect on electrons through the high plasma number-density and the Coulomb negative pressure. It is also observed from (4.5) that below a critical electron number-density, n_{0cr}, for a given atomic number, Z, the parameter T can become negative leading to an imaginary value for k_0 and consequently for the screening potential. Therefore, there is a lower plasma number-density bound, where the attractive force can exist. This is completely natural, since as the plasma density is lowered, the degeneracy limit of the Fermi–Dirac plasma is reached, beyond which the attractive force should disappear.

It is most surprising, however, to see some recent literature (Vranjes et al. 2012) to question such rigorously furnished theory as the quantum plasma theory and its fundamental applications, based on fallacious arguments. Also, based on the density functional theory computer simulations, some authors (Bonitz et al. 2012) have argued against the applicability of the linearized QHD theory and the existence of the Shukla–Eliasson attractive potential. One must note that the development of improved functional theory is currently a very active area of research, but it is far from clear whether the research will be successful in providing substantial increase in the accuracy desired (Schuch and Verstraete 2009). In the following numerical analysis it is confirmed that such attractive potential not only persists in high density matter but it also may be one of the essential ingredients causing strong ion-coupling in the cores of planets.

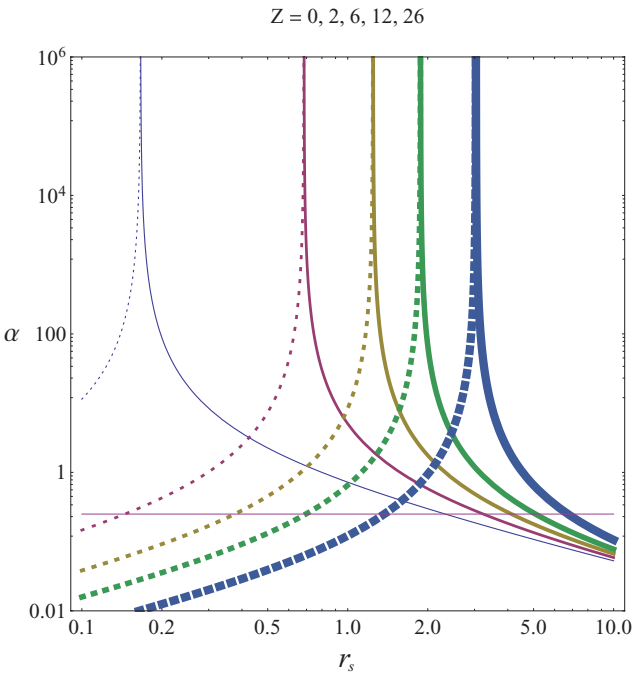


Figure 1. (Colour online) The phase-separation diagram of the Fermi–Dirac plasma without ($Z = 0$) and with Coulomb correction ($Z \neq 0$) in Log–Log scale. The horizontal line indicates the limit above (below) which the potential is attractive (repulsive). The solid/dashed branches show the imaginary/real parts of the phase diagram. The thickness of curves was used as a scale to show variation in the plasma atomic number.

6. Numerical analysis of phase-separation

Figure 1 shows the phase separation parameter, α, for the extended quantum plasma model in terms of the scaled fermion spacing parameter, r_s, for different values of the plasma atomic number. The figure consists of phase-separation curves for different plasma composition and each curve has two branches. It is observed that for the dashed branch the parameter T becomes negative and the potential imaginary. The solid branch, on the other hand, gives rise to the real electrostatic potential. The part of the phase-separation curve above the horizontal line indicates the presence of the Shukla–Eliasson attractive force and the part below indicates the horizontal line corresponding to the ordinary Debye screening potential. It revealed that as the plasma density increases (r_s increases) at some point, depending on the plasma atomic number, the attractive potential appears and by further increase in the plasma density (increase in r_s) at some point, depending on the plasma atomic

https://doi.org/10.1017/S0022377812000839 Published online by Cambridge University Press

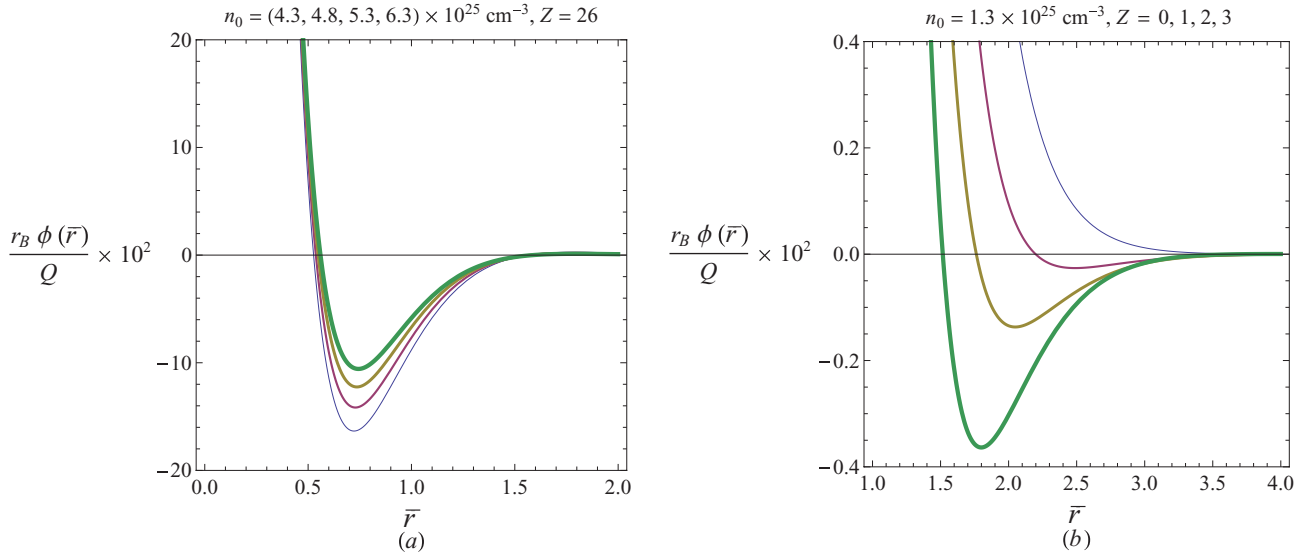


Figure 2. (Colour online) The variation of the Shukla–Eliasson attractive potential depth and scaled position with respect to change in the plasma number density (plot 2(a)) and atomic number (plot 2(b)) in the low-density plasma limit. The thin curves in each plot corresponds to the $Z = 0$ case and the thickness of curves was used as a scale to show variation in plasma atomic number and plasma number-density.

number, the attractive potential changes to the repulsive one. Note that at the critical point, $\alpha = \infty$, where attractive force is about to appear, the force between ions is the ordinary Coulomb force as expected. Also, at the point $\alpha = 1/4$, where the attractive force is about to disappear, the potential is finite and is as given in Shukla and Eliasson (2012). It is remarked from Fig. 1 that the starting and ending points for the attractive potential is strongly dependent on plasma composition and moves to larger densities for larger atomic number. This means that the attractive force in quantum plasmas starts and ends at higher plasma densities for higher atomic-number plasmas. It is also revealed that density range for which the attractive Shukla–Eliasson force exists narrows as the plasma atomic number increases. It is critical to note that the Shukla–Eliasson force for iron composition starts at an approximate density of $\rho \simeq 75.6675$ gr/cm^3, which is much higher than the zero-pressure solid iron with a density of around 8 gr/cm^3. This is an indication of the fact that the binding mechanism of the Shukla–Eliasson force, which is due to the electron tunneling and exchange interaction effects, is quite different from that of the ordinary solids. Figure 2 shows the characteristics of the attractive potential for various plasma parameters. It is remarked from Fig. 2(a) that the increase in the plasma number-density leads to the weakening of the attractive force for a given plasma number-density ($Z = 26$ for iron composition). As it was noted above, the attractive force for the iron-composed plasma happens at much larger densities than that of the ordinary solid iron (e.g., see Fig. 1(a)). It is also remarked from Fig. 1(a) that the ion separation in the Shukla–Eliasson quasi-lattice is almost independent of the plasma number-density variation. Figure 1(b) shows variation in potential profile parameters (the binding energy and the quasi-lattice parameter) due to change in the plasma composition parameter, Z. It is clearly observed that both binding energy and lattice parameters are altered significantly due to the change in the plasma atomic number. It is observed in Fig. 3(a) that the equilibrium distance, $\bar{r}_{\min}$, and the plasma binding energy (the depth of the potential minimum, $\phi(\bar{r}_{\min})$) increase strongly as the plasma density (or the reduced Wigner–Seitz radius) increases for all values of the atomic number, Z. Figure 3(b) further reveals that the plasma binding energy (the depth of the potential minimum, $\phi(\bar{r}_{\min})$) decreases strongly as the plasma density (or the reduced Wigner–Seitz radius) increases for all values of the atomic number, Z. However, it is remarked that the attractive potential occurs at higher densities for higher atomic number values. This can be an indication of the likelihood of the presence of heavier compounds at the cores of large planets like Jupiter in our solar system. Figure 3 also confirms that there are two (higher and lower) cutoff plasma density values for every given atomic number value which limit the occurrence of the Shukla–Eliasson attractive force. It is also observed that the attractive force starts closer to the test charge and with higher binding-energy values for higher atomic number of plasmas. The increase of plasma number-density is also observed to decrease ion separation, thereby leading to the formation of more compact with higher melting point quasi-lattices. Current research highlights features in super-dense degenerate plasma which can be of vital importance in the study of planetary sciences.

7. Concluding remarks

We used the linear dielectric response of a dense degenerate plasma of electron number-density in the range of that in the cores of big planets to show that the

https://doi.org/10.1017/S0022377812000839 Published online by Cambridge University Press

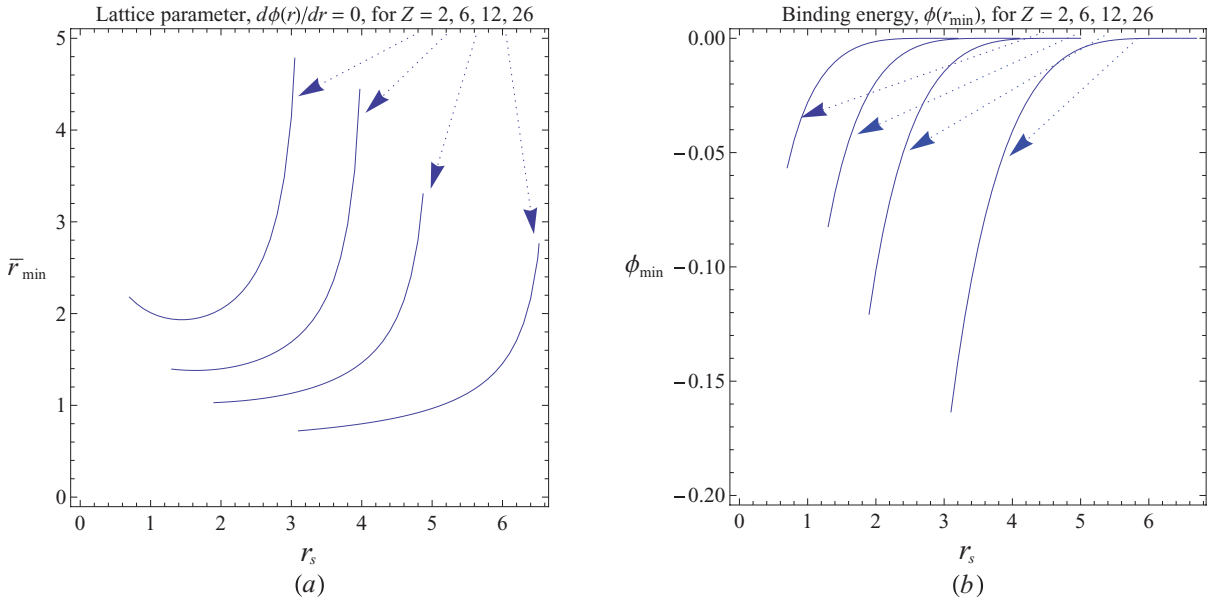


Figure 3. (Colour online) The regions and variation of attractive potential parameters, i.e., (a) the position of the potential minimum, $\bar{r}_{\min}$, and (b) the binding energy, $\phi(\bar{r}_{\min})$, for different values of the atomic number, Z in terms of the reduced Wigner–Seitz radius, r_s.

Shukla–Eliasson attractive force exists in such density regimes. It was found that the nature of the newly discovered attractive force in degenerate plasmas is quite different from those in ordinary solids and the binding length and strength in this density regime significantly depends on plasma density and composition. It was observed that heavier elements in the plasma give rise to stronger ion-binding. It was also remarked that the heavier the plasma ions the denser should be the plasma in order for the plasma binding to occur. This research highlights features which can be of fundamental importance in the study of the planetary core structures as well as inertial-confined laboratory plasmas.

Acknowledgements

The author expresses his deepest gratitude to Prof. Padma Kant Shukla for his generosity in exchanging his precious ideas. Insightful comments of anonymous referees which have led the paper to its current state are also truly appreciated.

References

Akbari-Moghanjoughi, M. 2010 Propagation and head-on collisions of ion-acoustic solitons in a Thomas–Fermi magnetoplasma: relativistic degeneracy effects. *Phys. Plasmas* **17**, 072101.

Akbari-Moghanjoughi, M. 2011a Remarkable paramagnetic features of Fermi-Dirac-Pauli plasmas. *Phys. Plasmas* **17**, 072702.

Akbari-Moghanjoughi, M. 2011b Propagation of arbitrary-amplitude ion waves in relativistically degenerate electron-ion plasmas. *Astrophys. Space Sci.* **332**, 187–192.

Akbari-Moghanjoughi, M. 2012a Comment on the article "Solitary waves and double layers in an ultra-relativistic degenerate dusty electron-positron-ion plasma". [*Phys. Plasmas* **19**, 033705, 064703.

Akbari-Moghanjoughi, M. 2012b Nonlinear excitations in strongly coupled Fermi-Dirac plasmas. *Phys. Plasmas* **19**, 042701.

Asenjo, F. A., Muñoz, V., Valdivia, J. A. and Mahajan, S. M. 2011 A hydrodynamical model for relativistic spin quantum plasmas. *Phys. Plasmas* **18**, 012107.

Bohm, D. and Pines, D. 1953 A collective discription of electron interactions: III. Coulomb interactions in a degenerate electron gas. *Phys. Rev.* **92**, 609–625.

Bonitz, M. Pehlke, E. and Schoof, T. 2012 On novel attractive forces between ions in quantum plasmas: failure of linearized quantum hydrodynamics. http://arxiv.org/abs/1205.4922. Accessed May 22, 2012.

Brodin, G. and Marklund, M. 2007 Spin magnetohydrodynamics. *New J. Phys.* **17**, 277.

Brodin, G. Marklund, M. and Manfredi, G. 2008 Quantum plasma effects in the classical regime. *Phys. Rev. Lett.* **100**, 3858.

Chandrasekhar, S. 1931 The highly collapsed configurations of a stellar mass. *Mon. Not. Roy. Astr. Soc.* **91**, 456–466; 1931 *Philos. Mag.*, **11**, 992; 1933 *ApJ* **74**, 81.

Chandrasekhar, S. 1939 *An Introduction to the Study of Stellar Structure*. Chicago, IL: The University of Chicago Press.

Chandrasekhar, S. 1953 The pressure in the interior of a star. *Mon. Not. R. Astron. Soc.* **113**, 667.

Chandrasekhar, S. 1984 On stars, their evolution and their stability. *Science* **226**, 497–505.

Crouseilles, N., Hervieux, P. A. and Manfredi, G. 2008 Quantum hydrodynamic model for the nonlinear electron dynamics in thin metal films. *Phys. Rev. B* **78**, 155412.

Fowler, R. H. 1926 On dense matter. *Mon. Not. Roy. Astr. Soc.* **87**, 114.

Gardner, C. 1994 The quantum hydrodynamic model for semiconductor devices. *SIAM, J. Appl. Math.* **54**, 409–427.

Haas, F. 2011 *Quantum Plasmas: An Hydrodynamic Approach*. New York: Springer.

https://doi.org/10.1017/S0022377812000839 Published online by Cambridge University Press

Haas, F., Eliasson, B. and Shukla, P. K. 2012 Relativistic Klein-Gordon-Maxwell multistream model for quantum plasmas. *Phys. Rev. E* **85**, 056411.

Haas, F., Garcia, L. G., Goedert, J. and Manfredi, G. 2003 Quantum ion-acoustic waves. *Phys. Plasmas* **10**, 3858.

Itoh, N., Kohyama, Y. and Takeuchi, H. 1987 Viscosity of dense matter. *ApJ* **317**, 733–736.

Kittel, C. 2008 *Introduction to Solid State Physics*, 8th Edn. New York: John Wiley.

Krall, N. A. and Trivelpeice, A. W. 1932 *Principles of Plasma Physics*. Columbus, OH: McGraw-Hill.

Levine, P. and Roos, O. V. 1962 Plasma theory of the many-electron atom. *Phys. Rev.* **125**, 207–213.

Lundin, J., Marklund, M. and Brodin, G. 2008 Modified Jeans instability criteria for magnetized systems. *Phys. Plasmas* **15**, 072116.

Manfredi, G. 2005 How to model quantum plasmas. *Fields Inst. Comm.* **46**, 263–287.

Manfredi, G. and Haas, F. 2001 Self-consistent fluid model for a quantum electron gas. *Phys. Rev. B* **64**, 075316.

Marklund, M. and Brodin, G. 2007 Dynamics of spin-1/2 quantum plasmas *Phys. Rev. Lett.* **98**, 025001.

Marklund, M., Brodin, G., Stanflo, L. and Liu, C. S. 2008 New quantum limits in plasmonic devices. *Europhys. Lett.* **84**, 17006.

Marklund, M. and Shukla, P. K. 2006 Nonlinear collective effects in photon-photon and photon-plasma interactions. *Rev. Mod. Phys.* **78**, 591–640.

Markowich, P. A., Ringhofer, C. A. and Schmeiser, C. 1990 *Semiconductor Equations*. New York: Springer-Verlag.

Mendonça, J. T. 2011 Wave kinetics of relativistic quantum plasmas. *Phys.Plasmas* **18**, 062101.

Nandkumar, R. and Pethick, C. J. 1984 Transport coefficients of dense matter in the liquid metal regime. *Mon. Not. R. Astron. Soc.* **209**, 511–524.

Pines, D. 1953 A collective discription of electron interactions: III. electron interactions in metals. *Phys. Rev.* **92**, 626–636.

Salimullah, M., Zeba, I., Uzma, Ch. and Jamil, M. 2009 Remarkable paramagnetic features of Fermi-Dirac-Pauli plasmas. *Phys. Plasmas* **16**, 033703.

Salpeter, E. E. 1961 Energy and pressure of a zero-temperature plasma. *ApJ* **134**, 669–682.

Schuch, N. and Verstraete, F. 2009 Computational complexity of interacting electrons and fundamental limitations of density functional theory. *Nature Phys.* **99**, 25001.

Shukla, P. K. and Eliasson, B. 2008 Screening and wake potentials of a test charge in quantum plasmas. *Phys. Lett. A* **372**, 2897–2899.

Shukla, P. K. and Eliasson, B. 2010 Nonlinear aspects of quantum plasma physics. *Phys. Usp.* **51**, 53; 2011 *Rev. Mod. Phys.* **83**, 885.

Shukla, P. K. and Eliasson, B. 2012 Novel attractive force between ions in quantum plasmas. *Phys. Rev. Lett.* **108**, 165007; 2012 *Phys. Rev. Lett.* **108**, 219902(E); 2012 *Phys. Rev. Lett.* **109**, 019901(E).

Shukla, P. K., Stenflo, L. and Bingham, R. 2006 Shielding of a slowly moving test charge in a quantum plasma. *Phys. Lett. A* **359**, 218.

Stenflo, L. and Shukla, P. K. 2010 Potential distribution around a charged dust grain in an electronegative plasma. *J. Plasma Phys.* **76**, 673.

Stenflo, L., Yu, M. Y. and Shukla, P. K. 1973 Shielding of a slow test charge in a collisional plasma. *Phys. Fluids* **16**, 450.

Tegeback, R. and Stenflo, L. 1975 Test charge potentials in turbulent plasmas. *Plasmas Phys.* **17**, 991.

Vranjes, J. Pandey, B. P. and Poedts, S. 2012 On quantum plasma: a plea for a common sense. *Euro Phys. Lett.* **99**, 25001.

https://doi.org/10.1017/S0022377812000839 Published online by Cambridge University Press